

Supplementary Information: Localization effect for doping and collaborative diffusion in Er^{3+} :YAG melt

Feng Liu¹, Xianjie Zhang², Kunfeng Chen³, Chao Peng¹, Guilin Zhuang², Dongfeng Xue^{1*}

1. Multiscale Crystal Materials Research Center, Shenzhen Institute of Advanced Technology, Chinese Academy of Sciences, Shenzhen 518055, China;

2. Institute of Industrial Catalysis, State Key Laboratory Breeding Base of GreenChemical Synthesis Technology, College of Chemical Engineering, Zhejiang University of Technology, Hangzhou 310032, P.R. China;

3. State Key Laboratory of Crystal Materials, Institute of Novel Semiconductors, Shandong University, Jinan 250100, China.

In this supplement materials, the radial distribution functions (RDF) between different atomic pairs, Al–O, Y–O, Al–Al, Y–Y, Al–Y, Al–Er, and Y–Er, in different doping concentration systems at temperature for 2000 and 2600 K have been shown, as well as the relationship between the average mean square displacement (MSD) and time for all ions in systems with doping concentrations of 3% and 5%. These are important supports for the conclusions in the main text.

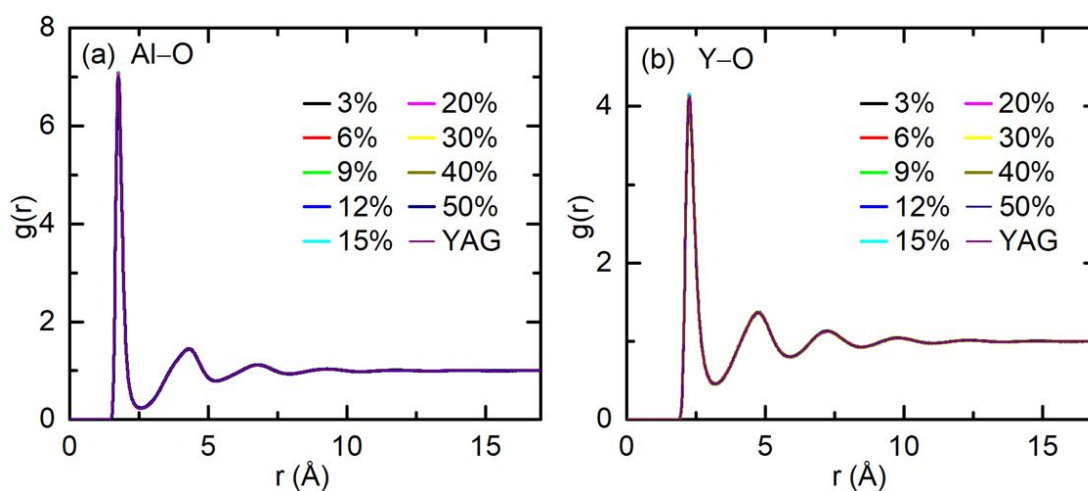


Fig. S1 The RDF for the Al–O (a) and Y–O (b) pairs in YAG melt (2000 K) with different concentration (at.%) of Er^{3+} .

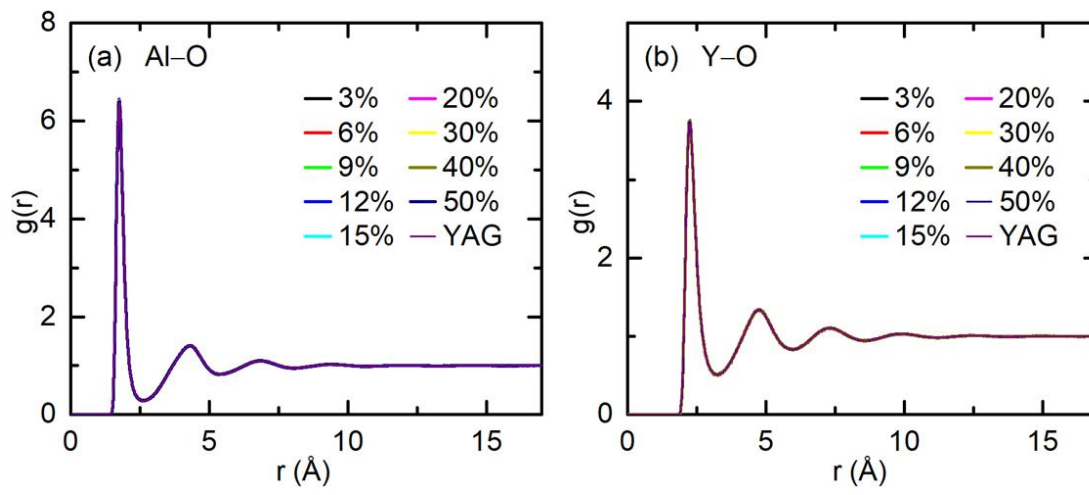


Fig. S2 The RDF for the Al–O (a) and Y–O (b) pairs in YAG melt (2600 K) with different concentration (at.%) of Er^{3+} .

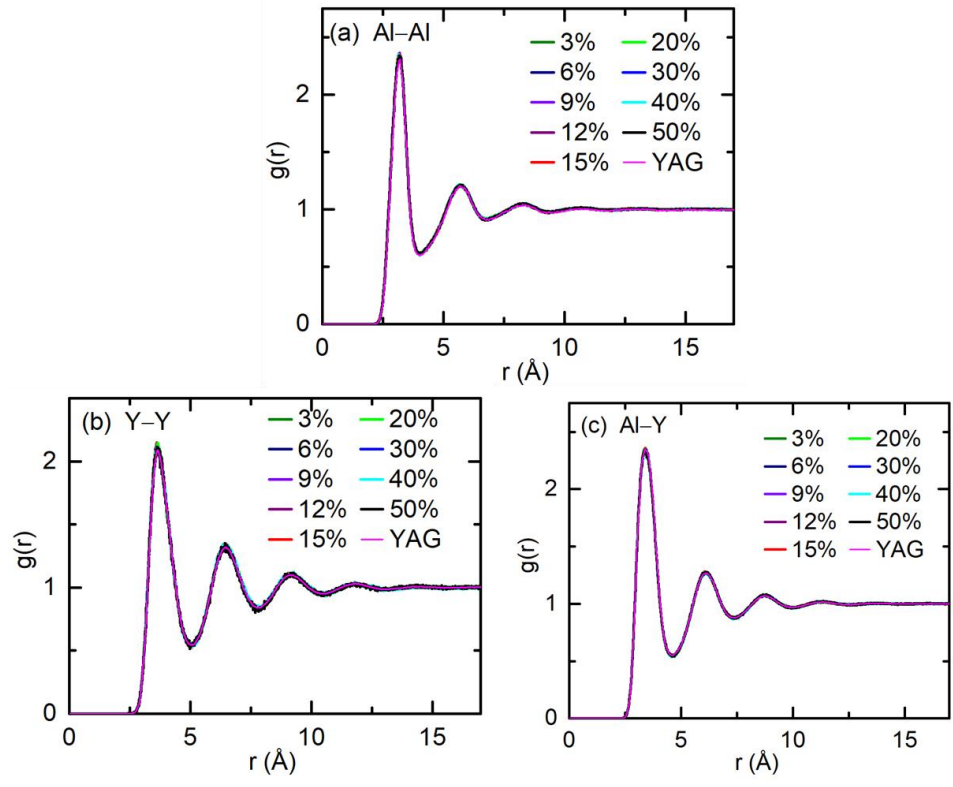


Fig. 3S RDF between Al–Al, Y–Y and Al–Y ionic pair in the YAG (2000 K) with 0, 3, 6, 9, 12, 15, 20, 30, 40 and 50 at.% Er.

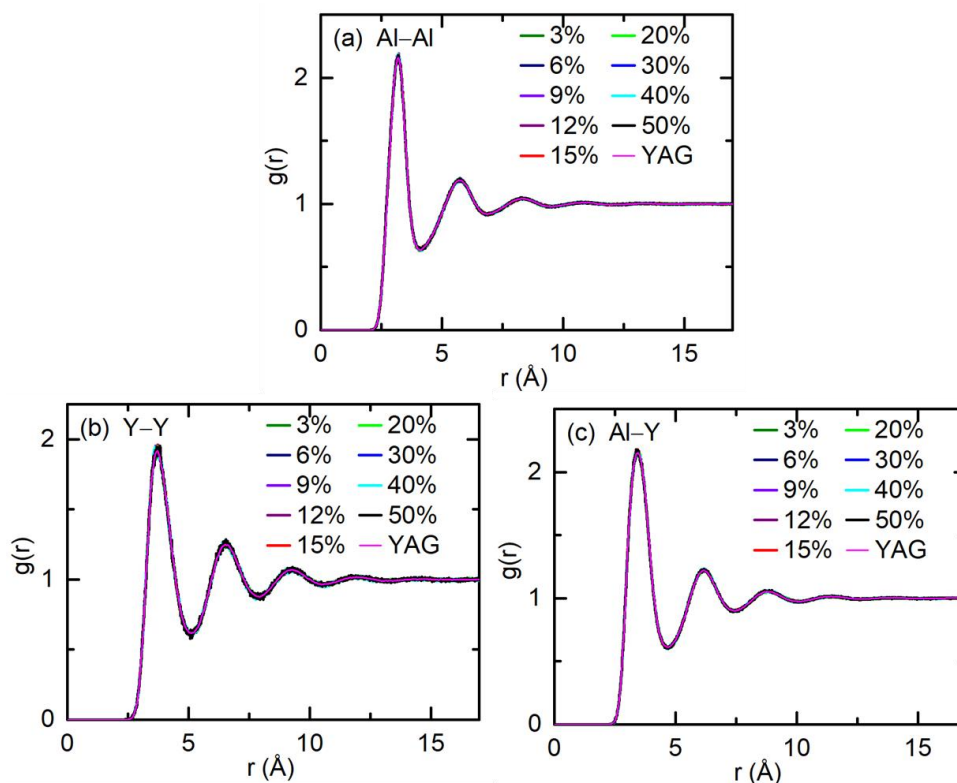


Fig. 4S RDF between Al-Al, Y-Y and Al-Y ionic pair in the YAG (2600 K) with 0, 3, 6, 9, 12, 15, 20, 30, 40 and 50 at.% Er.

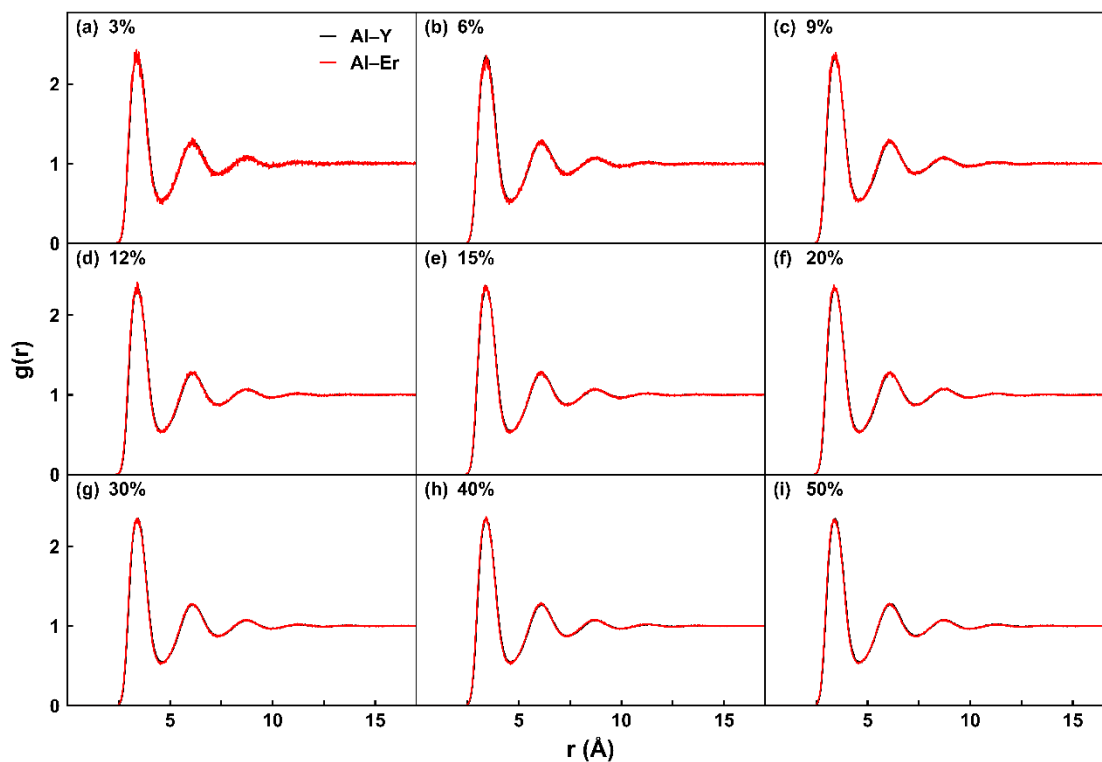


Fig. S5 RDF between Al-Y and Al-Er cation pairs in the melt (2000 K) with 3, 6, 9, 12, 15, 20, 30, 40, and 50 at.% Er.

20, 30, 40, and 50 at.% doping concentration.

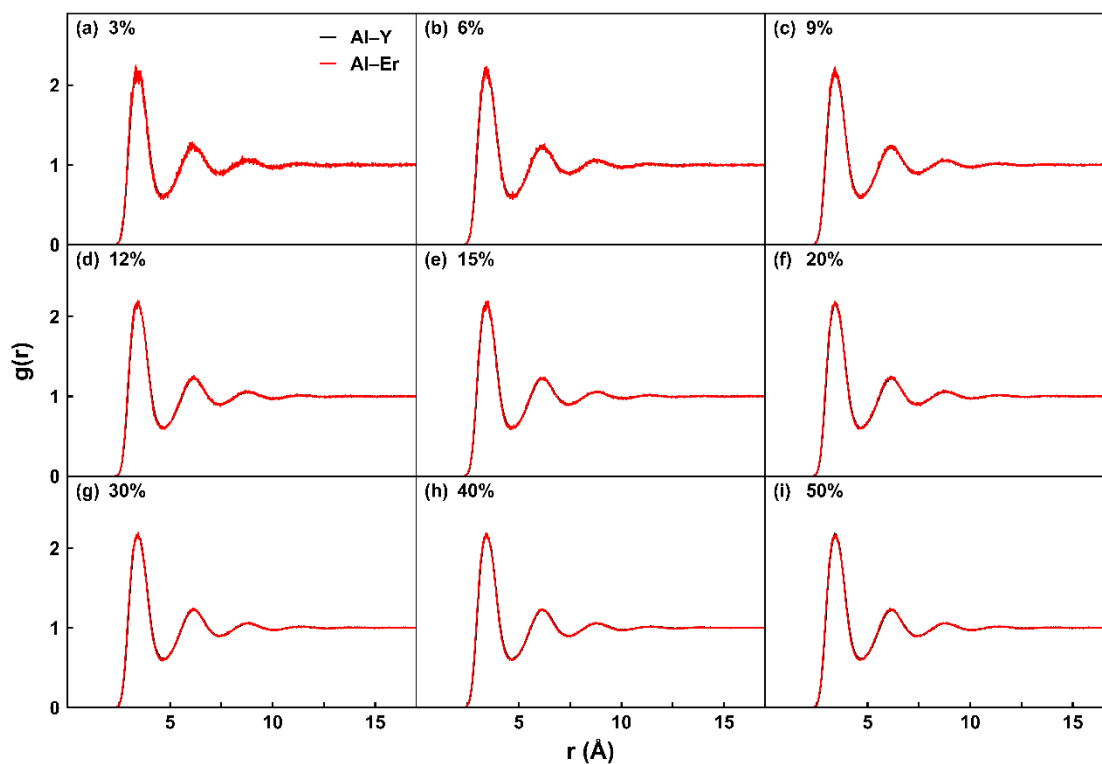


Fig. S6 RDF between Al-Y and Al-Er cation pairs in the melt (2600 K) with 3, 6, 9, 12, 15, 20, 30, 40, and 50 at.% doping concentration.

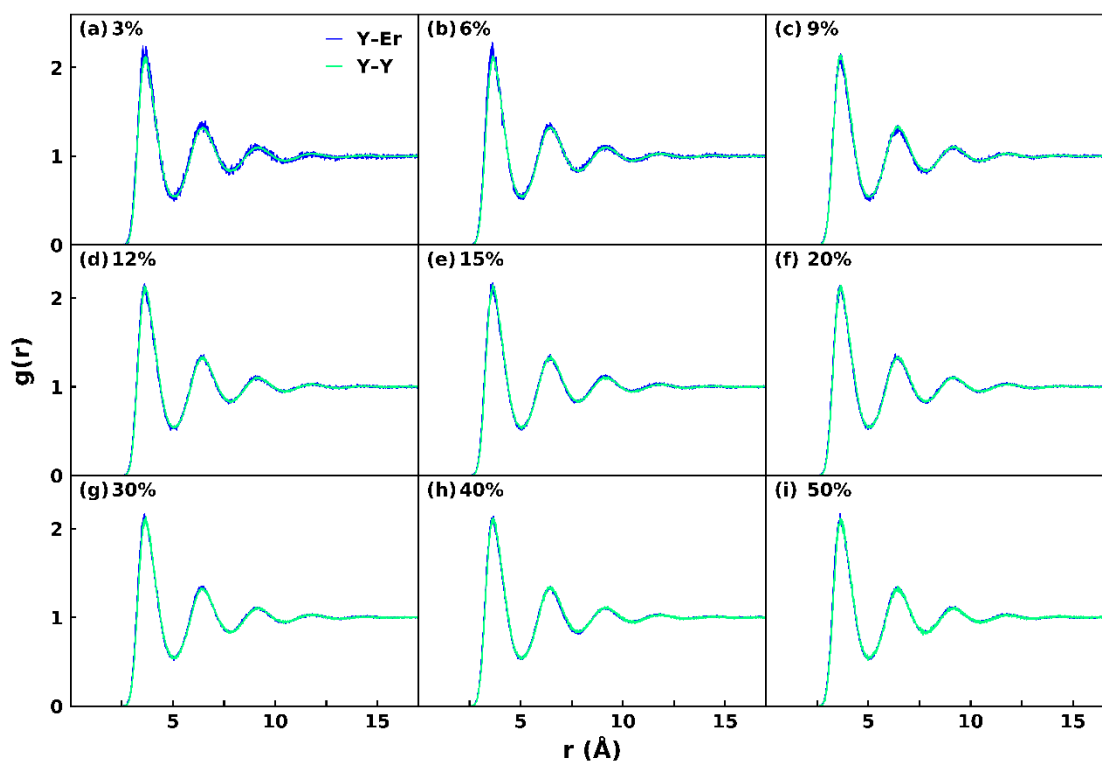


Fig. S7 RDF between Y-Y and Y-Er cation pairs in the melt (2000 K) with 3, 6, 9, 12, 15, 20, 30, 40, and 50 at.% doping concentration.

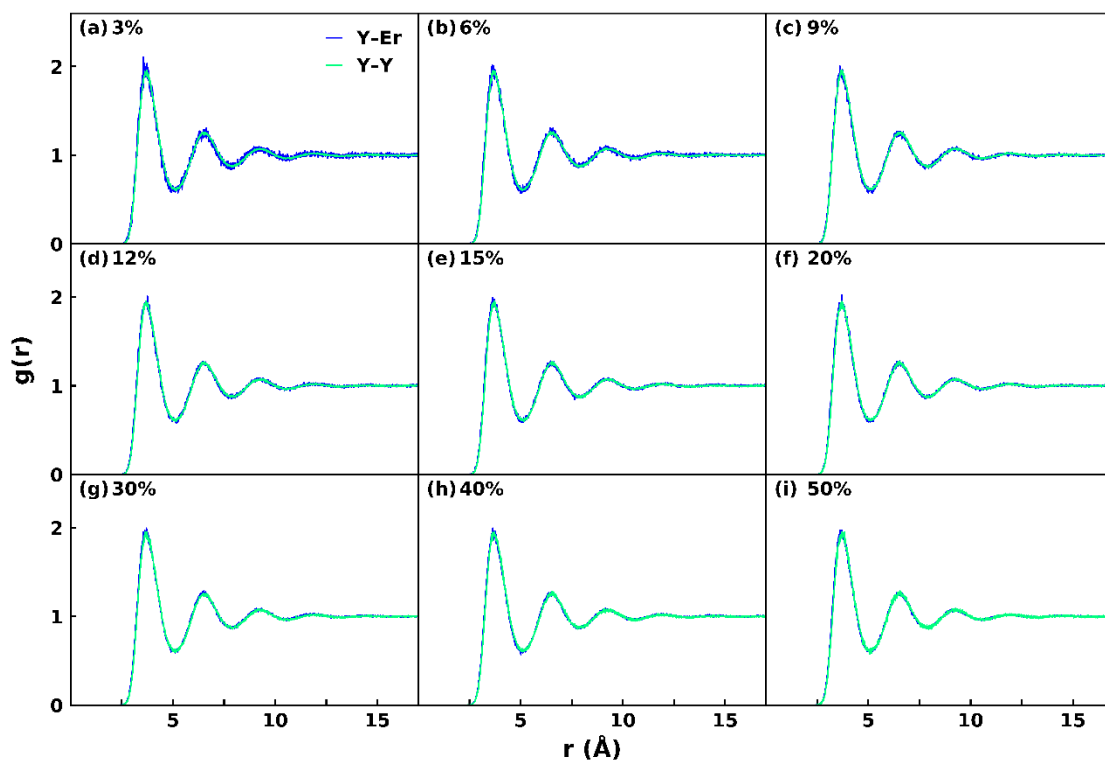


Fig. S8 RDF between Y–Y and Y–Er cation pairs in the melt (2600 K) with 3, 6, 9, 12, 15, 20, 30, 40, and 50 at.% doping concentration.

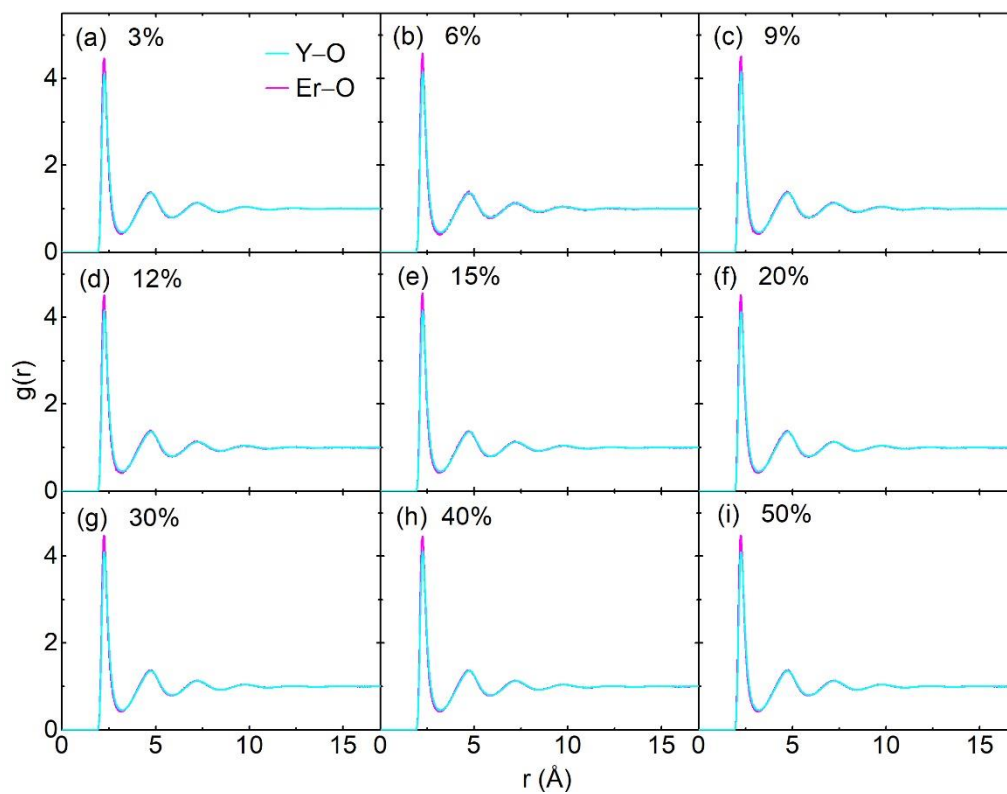


Fig. S9 RDF between Y–O and Er–O cation pairs in the melt (2000 K) with 3, 6, 9, 12, 15, 20, 30, 40, and 50 at.% doping concentration.

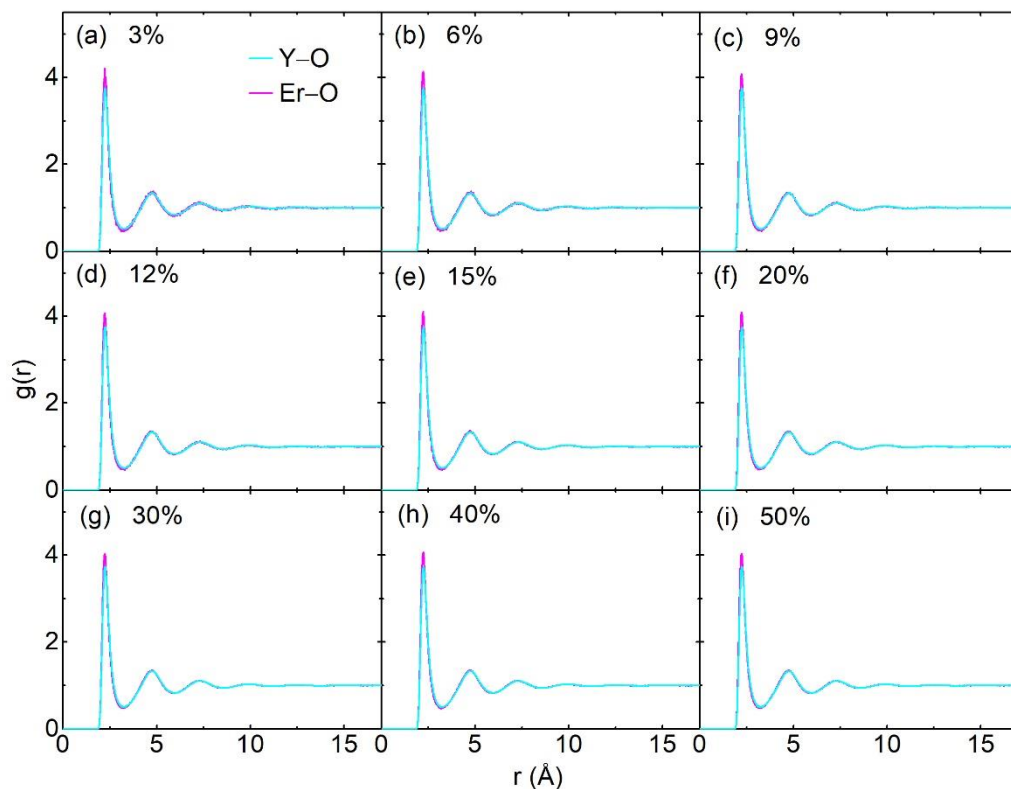


Fig. S10 RDF between Y–O and Er–O cation pairs in the melt (2600 K) with 3, 6, 9, 12, 15, 20, 30, 40, and 50 at.% doping concentration.

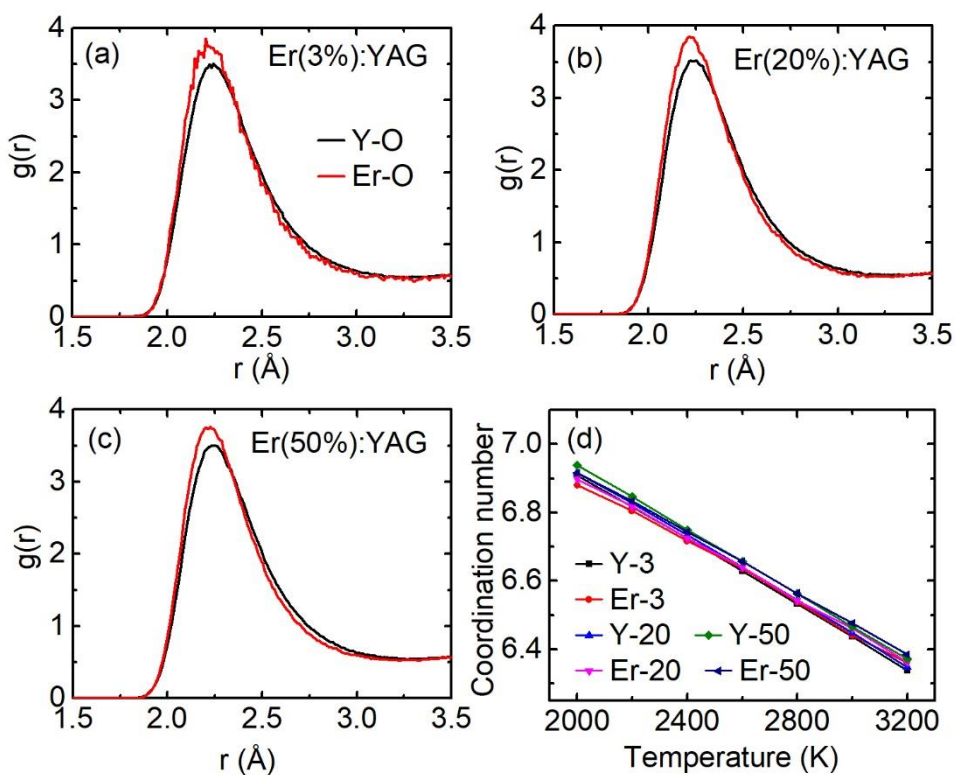


Fig. S11 (a), (b) and (c) represent the detailed first peak of ErO and YO RDF in systems with 3 , 20 and 50 at. % doping concentration respectively. (d) show the relationship between coordination number for Y^{3+} and Er^{3+} and temperature at these three doping concentrations.

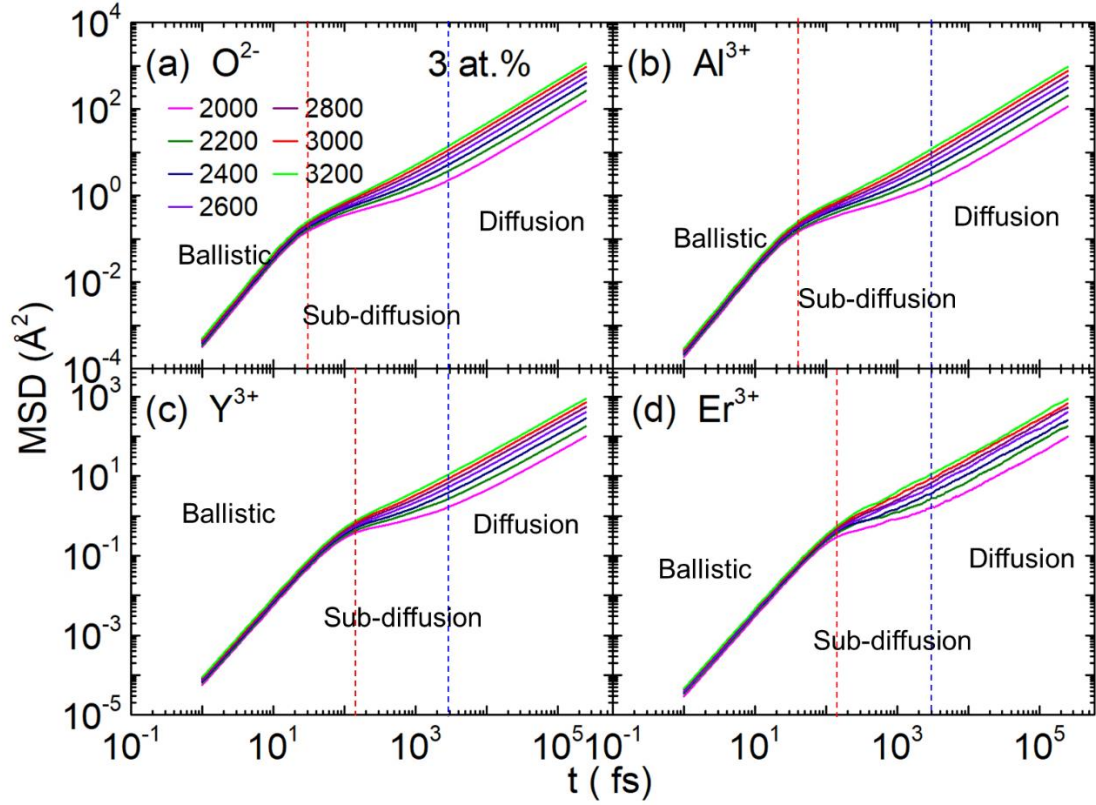


Fig. S12 Function of mean square displacement with time for O^{2-} , Al^{3+} , Y^{3+} , and Er^{3+} , which include three different dynamic stages in Er:YAG (3 at.%) melt at different temperature.

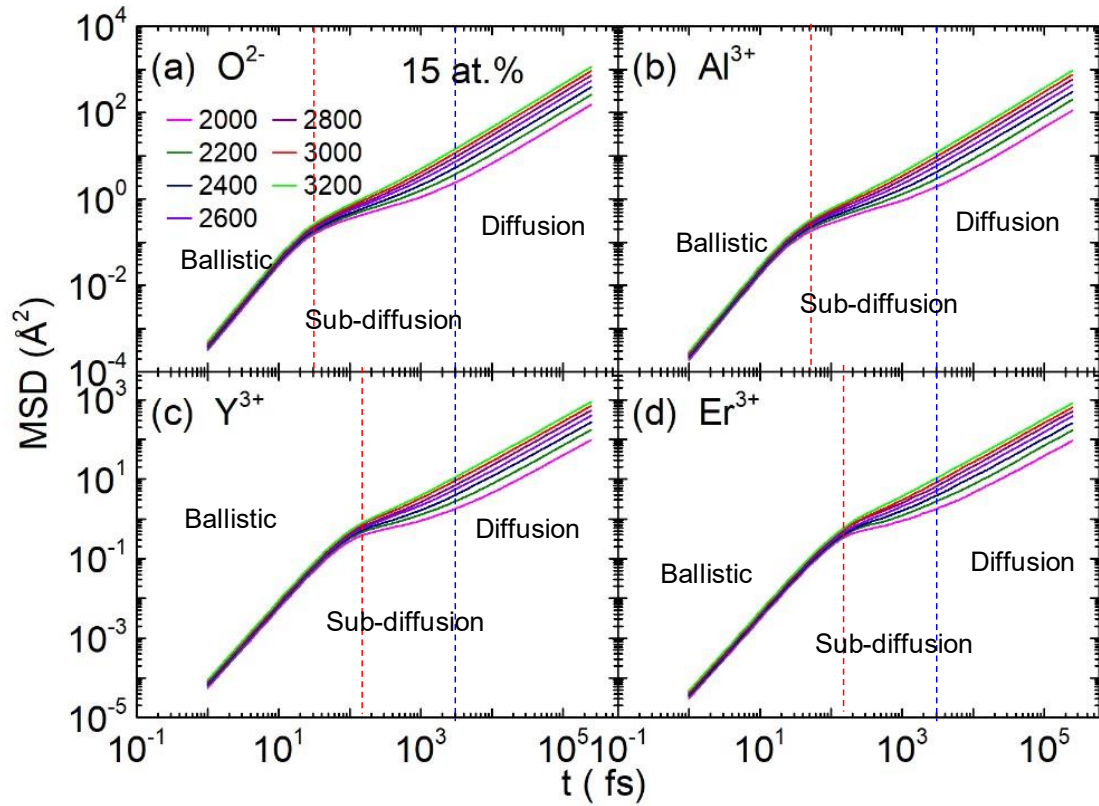


Fig. S13 Function of mean square displacement with time for O^{2-} , Al^{3+} , Y^{3+} , and Er^{3+} , which include three different dynamic stages in Er:YAG (15 at.%) melt at different temperature.

